The Cryosphere Discuss., 4, 429–467, 2010
www.the-cryosphere-discuss.net/4/429/2010/

The Cryosphere Discussions

This discussion paper is/has been under review for the journal The Cryosphere (TC).
Please refer to the corresponding final paper in TC if available.

A glacier inventory for the western Nyainqentanglha Range and Nam Co Basin, Tibet, and glacier changes 1976–2009

T. Bolch[1,5], T. Yao[2], S. Kang[2], M. F. Buchroithner[1], D. Scherer[3], F. Maussion[3], E. Huintjes[4], and C. Schneider[4]

[1]Institut für Kartographie, Technische Universität Dresden, Dresden, Germany
[2]Institute of Tibetan Plateau Research, Chinese Academy of Sciences, Beijing, China
[3]Institut für Ökologie, Technische Universität Berlin, Berlin, Germany
[4]Geographisches Institut, Rheinisch-Westfälische Technische Hochschule Aachen, Aachen, Germany
[5]Geographisches Institut, Universität Zürich, Zürich, Switzerland

Received: 5 March 2010 – Accepted: 16 March 2010 – Published: 1 April 2010

Correspondence to: T. Bolch (tobias.bolch@geo.uzh.ch)

Published by Copernicus Publications on behalf of the European Geosciences Union.

Abstract

The western Nyainqentanglha Mountain Range is located in the south-eastern centre of the Tibetan Plateau. Its north-western slope drains into Lake Nam Co. The area is of special interest for glacio-climatological research as this region is influenced by both the continental climate of Central Asia and the Indian Monsoon system, and it is situated at the transition zone between temperate and subcontinental glaciers. A glacier inventory for the whole mountain range was generated for the year ~2000 using automated remote sensing and GIS techniques based on Landsat ETM+ and SRTM3 DEM data. The change analysis is based on data from Hexagon KH-9 and Landsat MSS (year 1976), Metric Camera (year 1984), and Landsat TM/ETM+ (1991, 2001, 2005, 2009). Manual adjustment was especially necessary for the panchromatic Hexagon data and for debris-covered glaciers. The whole mountain range contains about 960 glaciers covering an area of $795.6 \pm 22.3\,\text{km}^2$ while the ice in the drainage basin of Nam Co covers $198.1 \pm 5.6\,\text{km}^2$. The median elevation of the glaciers is ~5800 m a with the majority terminating around 5600 m. Five glaciers with debris-covered tongues terminate lower than 5200 m. The glacier area decreased between 1976 and 2001 by about $6 \pm 3\%$, which is less than presented in previous studies based on topographic maps from the 1970s and Landsat data from 2000. Glaciers continued to shrink during the period 2001–2009. No advancing glaciers were detected. Detailed length measurements for five glaciers indicate a retreat of the tongues of around 10 m per year (1976–2009) with higher absolute but lower relative values for the larger glaciers.

1 Introduction

Often described as Asia's "water tower", the Tibetan Plateau (TiP) is the source of many major rivers (e.g. Brahmaputra, Ganges, Huang He, Indus, Mekong) and essential to millions of people living in the surrounding regions. Glaciers on the TiP are characteristic elements of the natural environment and significantly contributing to its

TCD

4, 429–467, 2010

Title Page
Abstract | Introduction
Conclusions | References
Tables | Figures
◀| |▶
◀ ▶
Back | Close
Full Screen / Esc
Printer-friendly Version
Interactive Discussion

water resources. Like in many other parts of the world the TiP's climate shows a significant temperature increase latest since the mid 1950s (Liu and Chen, 2000, Frauenfeld et al., 2005, Kang et al., 2010), accompanied by an increase of precipitation (Zhao et al., 2004, Liu et al., 2009), while glaciers receded almost throughout the entire Tibetan Plateau during recent decades (Ding et al., 2006, Ye et al., 2006, Xiao et al., 2007, Li et al., 2008). This trend is also confirmed for the western Nyainqentanglha range (Kang et al., 2007, Yao et al., 2007, Wu and Zhu 2008, Frauenfelder and Kääb, 2009). Recent glacier wastage has not only caused an increase in river run off from the plateau but also rising lake levels (Yao et al., 2007). However, it has to be taken into account that further glacier melt is likely to result in a decrease of run-off (Braun et al., 2000, Hagg et al., 2006). Therefore, glacier changes have major impact on the human lives and activities, as well as on flora and fauna (Beniston, 2003). In addition, glacier recession often results in an increasing threat from natural hazards such as landslides and glacial lake outburst floods (Haeberli and Beniston, 1998, Richardson and Reynolds, 2000, Bolch et al., 2008a, Bajracharya and Mool, 2009). This has also been observed in Tibet (Ma et al., 2004). Glaciers itself are important climate proxies in mountainous areas where climate stations are rare or non-existent. Amdo, situated at 4820 m, is currently the highest permanent climate station on the TiP (Liu et al., 2009), whereas the snow-line elevation increases from about 4800 m in the humid south-eastern part to over 6200 m in the extremely continental north-eastern parts of the TiP (Shi et al., 1980).

According to Huang (1990) glaciers on the TiP are roughly classified into continental or subpolar and maritime or temperate glaciers. Continental type glaciers with little precipitation and low ice temperatures are widely distributed from the central to the north-western plateau, while the maritime type with high monsoon precipitation and a temperate ice body is limited to the humid south-eastern region (Fujita et al., 1996, Fujita and Ageta, 2000). In the transition zone between continental and maritime glaciers the polythermal type with both cold and temperate areas within the glacier body is common. As the Indian summer monsoon influences most Tibetan glaciers, they belong to the "summer-accumulation type" after Ageta and Higuchi (1984), with the maximum of annual accumulation and ablation occurring simultaneously in summer (Ageta and Fujita, 1996, Kang et al., 2009).

Multi-temporal and multi-spectral satellite data are ideal to study glacier changes simultaneously for larger areas in remote mountainous terrain as they allow automated glacier mapping. A simple but robust method is the use of ratio images using one visible or near infrared and one short wave infrared band (Bolch and Kamp, 2006, Paul et al., 2009). The earliest imagery suitable for automated mapping is available since the launch of Landsat TM in 1982.

The availability of digital elevation models allows to split contiguous ice masses into their drainage basins, and to obtain several characteristic variables of the glaciers (e.g., minimum, maximum, median elevation, slope, aspect) automatically (Schiefer et al., 2008, Paul et al., 2009, Bolch et al., 2010). Declassified imagery from the American intelligence satellite missions such as Corona KH-4, Corona KH-4B and Hexagon KH-9 with the first images available in the early 1960s is ideal to extend the analysis back in time (Bolch et al., 2008b, Narama et al., 2006, Surazakov and Aizen, 2010).

Our study area, the western Nyainqentanglha range, situated in the south-eastern centre of the TiP (Fig. 1), is of special interest for several reasons:

- a) It is under the complex influence of both the continental climate of Central Asia and the maritime monsoon,
- b) It comprehends glaciers of subcontinental (subpolar) and polythermal characteristics (Shi and Liu, 2000),
- c) It contains several glaciers where length measurements are existing (Kang et al., 2007), one glacier where mass balance measurements where started (Kang et al., 2009), and parts of the study area drain into a large lake (Nam Co) that is well studied (Wu and Zhu, 2008, Schütt et al., 2008).

However, there is to our knowledge currently no paper available addressing all glaciers and their changes in the western Nyainqentanglha Range for more than two points in time in detail. Therefore, the aims of this study are

- a) to generate a glacier inventory for the whole mountain range, and to provide information on the general glacier characteristics,
- b) to evaluate the data from the 1970s based on the topographic maps using declassified imagery,
- c) to analyse glacier changes from the 1970s until ~2000 for the whole mountain range, and for the Nam Co Basin,
- d) to analyse glacier variability for a representative subset of glaciers in detail.

2 Study area

The western Nyainqentanglha represents a SW-NW striking high-mountain range of approx. 230 km in length with heights between some 5000 and 7162 m (Mount Nyainqentanglha), which is bordered to the SE by the Yangbajain-Damxung Valley (cf. Yao, 2008), and to the NW by Lake Nam (Nam Co, 4725 m, Fig. 1), Tibet's largest salt water lake with noticeable variations in size since the Last Glacial Maximum (Schütt et al., 2008), and also within the last 30 years (Wu and Zhu, 2008, Chen et al., 2009). The mountain chain is characterised by crystalline rocks and tectonically controlled transverse valleys and cirques (Yang et al., 1986, Ren et al., 1987).

Relatively few is known on the regional mountain climate because of its high elevation and the subsequent lack of long-term observational data. However, assumptions can be made aided by the nearby meteorological stations and the recent installation of observational instruments on Zhadang Glacier and the nearby Nam Co station (You et al., 2007). The climate is characterised by a strong seasonality in both temperatures and precipitation. Summer temperatures on Zhadang Glacier (elevation ~5600 m) observed by Kang et al., (2009) are between 0.35 and 1 °C. Following Sato (2001), summer mean temperatures are expected to be around 3 °C at the same elevation, illustrating the cooling effect of glaciated areas. Winter temperatures at this altitude should stay below −15 °C. Annual precipitation measured at the Nam Co station (elevation ~4725 m) is 414.6 mm during the past three years, and concentrates in the warm season (90% of the annual precipitation is observed between May and September) (Zhang et al., 2008). Chen et al. (2009) suggest an increase of annual precipitation in the Nam Co region.

According to Shi and Liu (2000) the glaciers of the mid-east section of the Nyainqentanglha Range receive abundant summer monsoon precipitation, resulting in temperate (maritime type) glaciers, whereas the western Nyainqentanglha Range, the area of the authors' major interest, carries subcontinental (subpolar) and polythermal glaciers. These glaciers are located in a continental summer-precipitation climate. The formation of superimposed ice plays an important role in glacier mass balance as it prevents mass loss during the ablation season due to the retention of meltwater (Ageta and Fujita, 1996, Fujita et al., 2007). Additionally, monsoonal summer snowfall leads to increasing surface albedo and largely restrains ablation. These glaciers can therefore maintain their mass even under arid conditions with strong solar radiation (Fujita and Ageta, 2000, Kang et al., 2009).

3 Data and methods

3.1 Data

The main source for the glacier inventories are Landsat scenes from different years (Table 1). One scene covers almost the entire mountain range and is available for free from different sources (e.g. USGS, http://glovis.usgs.gov/ and the Global Landcover Facility, GLCF). Most of the scenes from the USGS are orthorectified in best available level (1T) and well co-registered. In addition, the level 1T data showed a better fit (deviation < 30 m) than the Landsat data from GLCF (which are geocover-terrain corrected, Tucker et al., 2004) to our non differential GPS-data. No DGPS data are available for this study. We selected a Landsat ETM+ scene of the year 2001 from the USGS as reference. Almost no shift was observed for the ETM+ scenes, whereas the TM scenes had small shifts of 15 to 20 m. Unfortunately, no suitable scene for the time around 1990 was available. We found only one scene from 1991 at GLCF with some seasonal snow cover. For this scene, a shift of about two pixels (60 m) and some deviations at mountain ridges were observed. Hence, we shifted the scenes for a better fit to the USGS data. Fortunately, the main area of interest around Mt. Nyainqentanglha and Zhadang Glacier is in the centre of the ETM+ scenes almost not affected by scanline errors present in ETM+ images since early summer 2003. Nevertheless, we had to use several scenes with the scan line error ("SLC-off" scenes) for each year due to different snow conditions, cloud cover and the data gaps. A typical scene is shown in Fig. 2. We utilized Hexagon KH-9 data from the year 1976 to extend the coverage back in time and to evaluate the exisiting data from the Chinese Glacier Inventory (CGI, Li, 2003). This panchromatic spy imagery data has a resolution of about 8 m, and a footprint of about 120 by 240 km. One scene covers almost the entire mountain range. Most glaciers in the south-western part are identifiable due to low seasonal snow cover. However, the margins of some smaller high-altitude glaciers are hardly to identify correctly due to low contrast. Hence, we used Landsat MSS data from the same year as additional information. Unfortunately, this scene has also partly higher seasonal snow cover. Additional information was provided by Corona data from 1970 with a resolution of 4 m, and by Space Shuttle Metric Camera (MC) images (Konecny et al., 1984) from the year 1984 with a resolution of ~20 m. Table 1 provides an overview of the utilized scenes.

We co-registered the other scenes to the USGS scene from 2001, if the shift exceeds 15 m. The spatial reference was WGS84, UTM Zone 46N. The Hexagon, Corona, and Metric Camera data had to be orthorectified as no terrain correction was applied to these data yet. The ETM+ images were pan-sharpened for visual checking and improvement. We orthorectified and co-registered the KH-9, MC and KH-4B imagery in a two-folded step using ERDAS Imagine software: The projective transformation based on selected ground control points (GCPs) and the SRTM3-DEM was performed, followed by spline adjustment. In total, we used 95 GCPs for the KH-9, 25 GCPs for KH-4, and 39 for the MC imagery.

We needed a suitable DEM not only for orthorectification but also for the calculation of glacier parameters and to split the glaciers into their drainage basins. No detailed DEM was available for the study area. Therefore, we downloaded and tested SRTM3 data (90 m resolution) from different sources (USGS, GLCF, CIGAR) and the ASTER GDEM (30 m resolution). The registration of the ASTER GDEM was suitable as it matches the reference USGS Landsat scene with a deviation of less than 30 m. The main disadvantage is that it contains several holes, and does not represent well the areas of steep slopes. These phenomena are common for DEMs derived from ASTER data (Kamp et al., 2005, Toutin 2008), and are likely due to the availability of few scenes only in our study area. However, quality of ASTER GDEM is improving, and a better DEM can be expected in the future. The SRTM DEM is known to be of good accuracy (Falorni et al., 2005), and has also the advantage that it is more accurate in areas of low contrast (e.g. due to snow). Visual checks confirmed this also for the study area. Surprisingly, the SRTM3 data from different sources, which we projected to UTM to match the satellite images, had a shift of about two pixels to each other. The best fit with a deviation of less than one pixel to the USGS Landsat reference scene showed the void filled CIGAR SRTM, vers. 4 (http://tm.cigar.org).

3.2 Glacier identification

Due to the size of the study area and the multi-temporal coverage, we applied a semi-automated approach to produce glacier outlines using Landsat TM/ETM+ imagery. We selected the TM3/TM5 band ratio to be most appropriate for glacier mapping based on previous experience (Bolch and Kamp, 2006; Bolch et al., 2010) and the recommendations for the compilation of glacier inventories (Paul et al., 2009). In addition, a 3 by 3 median filter was performed, which only marginally alters the glacier size but eliminates holes of one pixel. These are usually misclassified pixels due to debris or boulders on the glacier (Paul et al., 2002). We visually checked glacier polygons derived from our ratio method for gross errors, and manually improved them where necessary. Debris-covered ice, proglacial lakes, seasonal snow, and, for the SLC-off scenes, data gaps represented major sources of misclassified areas. The termini of some debris-covered glaciers were hardly or not identifiable by Landsat imagery. Here, we used the ETM+ panchromatic sharpened image to identify the correct margin. The higher resolution Hexagon and Corona imagery (Fig. 3) helped in this process.

According to the recommendations to obtain a global glacier coverage for the year around 2000 (Paul et al., 2009), we generated in the first step an inventory for the whole southern mountain range based on the Landsat ETM+ scene from the 6th December 2001. We used the other scenes from 2001 and 2000 as additional information in case of cast shadow and higher seasonal snow cover. High seasonal snow hampered the correct mapping of the glaciers in the northern part. We had to use the three scenes from 2009 for this area due to clouds and the data gaps from the scan line error. Finally, full spatial coverage could be obtained. We manually adjusted the ~2001 outlines to the situation in 1976 based on the panchromatic Hexagon data, and used the MSS data as additional information. No multi-temporal inventory could be generated for the north-eastern part of mountain range (Fig. 1) due to unsuitable snow cover on both the Hexagon and the MSS data. The 2009 inventory for the detailed study area was generated semi-automatically as described above.

Five selected glaciers (Panu, Lalong, Xibu, Zhadang, and Tangtse Glacier No. 2) were studied in detail. The selection is based on existing studies that could be used for comparison (Kang et al., 2007). We manually adjusted the outlines for the additional years 1991 and 2005, and for Xibu and Lalong Glacier for the additional year 1984. High seasonal snow cover on the 1984 Metric Camera data hampered the correct delineation of other smaller glaciers.

In a first step, we limited the size of mapped glaciers to those larger than 0.01 km^2. However, we limited the comparison of glacier areas to those larger 0.1 km^2 as seasonal snow on at least one of the utilized scenes hampered the correct delineation, thus high errors would be introduced. Even, if a scene seems to be suitable, higher errors could be introduced to a scene or section with no seasonal snow. E.g., we observed a difference in area of about 13% for a small glacier (~0.15 km^2) for two different scenes from the same year (Fig. 4).

We could not find a single glacier that advanced between 1976 and 2001. Hence, we clipped all glaciers to the 1976 extend. The use of this mask ensured that the upper glacier boundary and the margins of the nunataks were kept constant, and no error would be introduced due to varying seasonal snow cover or different ice divides.

3.3 Glacier inventory and change analysis

The contiguous ice masses had to be divided into their drainage basins in order to obtain a glacier inventory. We followed the automated approach presented by Bolch et al. (2010), and derived the basins based on hydrological analysis within a one-kilometre-buffer around each glacier. The SRTM3 DEM was suitable to detect correct flow divides on ice fields. The main drawback, however, was the location of some steep mountain crests. They differed sometimes by approximately one pixel (90 m) from the location in the satellite imagery. An additional error occurred when smaller glaciers connected in parts of the accumulation area are close to larger ones so that no own basin was generated automatically. Hence, we manually improved the basins based on the satellite imagery. This method was superior to the fully manual method as many ice divides were calculated correctly.

An identification number was assigned to each glacier based on the 1976 extends. We treated all ice masses as a single glacier also in cases where glaciers separated from each other in order to allow subsequent change analysis. The following characteristic parameters were obtained for each glacier based on the SRTM3 DEM: minimum, maximum and median elevation, mean slope, aspect, and the surface area.

3.4 Error estimation

The potential error of the multi-temporal analysis mainly arises from positional and mapping errors. Visual checks of (almost) stable landforms like mountain peaks or lateral moraines on the co-registered imagery resulted in a mean deviation of one pixel or less for the TM scenes (<30 m), and less than half a pixel for the ETM+ scenes (<15 m). Some ETM+ scenes from the USGS matched perfectly. Co-registration error of the Hexagon image was higher due to the more complex image geometry. The error was about two pixels (20 m) for the detailed study area, and could be up to four (40 m) at the outer part of the imagery where fewer tie points (TPs) were collected. The uncertainty of glacier mapping depends on the resolution of the utilised imagery and the conditions at the time of the acquisition (especially seasonal snow). Under best conditions sub-pixel accuracy of less than half a pixel can be achieved. We estimated the uncertainty by the buffer method suggested by Bolch et al. (2010) and Granshaw and Fountain (2006). We have chosen a buffer size of 10 m for the Hexagon image, and 7.5 m for the ETM+ images. This leads into an uncertainty of 3.5% for the Hexagon imagery, and 2.8% for the ETM+ images.

4 Results

4.1 Glacier characteristics

The whole mountain range contains almost 1000 glaciers according to our inventory. However, glacier counts are vague and depend on the purpose; e.g. contiguous ice masses can be counted as single entities, or can be subdivided into multiple glaciers as we did where parts of the ice masses cross ridges. Glaciers of the western Nyainqentanglha Range cover an area of about 800 km^2, while little more than 100 km^2 are situated in the north-eastern section, which is not further investigated. Ice coverage of the area around Mt. Nyainqentanglha and of the Nam Co drainage basin is each little less than 200 km^2 (Table 2).

The highest number of glaciers can be found in the size class 0.1–0.5 km^2, whereas glaciers between 0.5–1.0 km^2 cover the largest area (Fig. 5a). The predominant aspect of the glaciers is north (Fig. 5b).

The median elevation of the glaciers, which is often taken as the best estimation for the long-term ELA, is situated at around 5820 m. The majority of the glaciers terminate at around 5600 m. Only five glaciers terminate lower than 5200 m, with the lowest elevation at 5130 m. These glaciers are all debris-covered at their tongues. Characteristics of the five glaciers investigated in detail are shown in Table 3.

The calculated area and length differ partly from previous published data such as the data from the Chinese Glacier Inventory (CGI) from the 1970s which is available through the GLIMS database (Li 2003). The main reasons for the deviation are different interpretation of ice divides, debris-cover and contributing glaciers as well as glacier shrinkage since the 1970s. In addition, we found a notable shift in location of some glaciers of the CGI which was also mentioned by Frauenfelder and Kääb (2009).

4.2 Glacier shrinkage/recession

Ice cover in the south-western study area diminished from 734.1 ± 25.7 to 692.4 ± 19.4 km^2 by 41.7 ± 22.4 km^2 or 5.7 ± 3.1% (0.23 ± 0.12%/a) in the period 1976–2001. The percentage loss and the rate for Nam Co drainage basin and the detailed study area around Mt. Nyainqentanghla are in the similar range but little higher for the first, and a little lower for the latter (Table 4). The shrinkage rate for the period 2001–2009 is higher than for 1976–2001 but not statistically significant given the higher error term. However, visual checks and detailed analysis confirm ongoing glacier shrinkage and retreat between 2001 and 2009 (Fig. 6 and Table 4). The overall number of glaciers remained almost unchanged. The disappearance of very few glaciers is compensated through disintegration of others.

Analysis of the relative area change against the initial glacier area indicates greater percentage loss for smaller glaciers. However, there is a large scatter especially with smaller ones and there are glaciers which did not shrink in all size classes (Fig. 7a). The absolute area loss is higher for larger glaciers (Fig. 7c). There is a small tendency that glaciers with lower median elevation lost relatively more area than higher elevation glaciers (Fig. 7b) whereas the highest absolute area loss is attributed to elevations around 5800 m, which is about the median elevation of all glaciers.

Analysis of the glacier hypsometry shows that ice coverage above 6000 m remains almost unchanged while the highest absolute ice loss occurs between 5500 and 5700 m (Fig. 8). The overall characteristics of glacier hypsometry did not change much between 1976 and 2001.

Detailed analysis of the five selected glaciers confirms the above mentioned tendencies. All glaciers decreased continuously both in area and length throughout all investigated periods (Table 5). The rate of area loss is significantly higher for three glaciers in the period 2001–2009 compared to 1976–2001, whereas the rate is similar for Panu Glacier, and an opposite tendency for Lalong Glacier could be found. Length changes show similar behaviour. Absolute area loss varies between 0.24 km^2 (Tangtse Glacier No. 2, one of the smallest glaciers) and 0.44 km^2 (Xibu Glacier, the largest one) for 1976–2009 while the percentage loss is highest for Zhadang Glacier (14.2%, the smallest glacier studied), and lowest for Xibu Glacier (1.9%). There is a slight tendency that retreat rates 1976–1991 are higher than those from 1991 to 2001 but lower than those from 2001 to 2009. One glacier contributing to the main Panu Glacier in 1976 separated from it in 2001 (Fig. 9).

5 Discussion

5.1 Images and methodology

The spaceborne imagery listed in Table 1 enables us setting up a glacier inventory of the western Nyaingentanglha Range, and to trace back changes in glacier extension over a period of more than 40 years. This represents one of the longest time series over which a change detection of the glacier coverage has been performed until present. Although several data sets allow for a determination of the volume change due to their stereo capabilities, only length and area variations have been calculated so far. Especially the Hexagon KH 9 imageries from 1976 are of great value for analysis of glacier changes over a longer time period. They are superior to Corona KH-4A or KH4B, which were acquired, in most cases, only some years earlier but have a far less coverage (~20×120 km to 120×240 km). In addition, higher distortions make them much more difficult to georectifiy/co-register. However, the earliest Corona imagery successfully applied to trace glacier changes date back to the beginning of the 1960s (Bolch et al., 2008b). Corona KH-4 imagery from the 1960s is available but unfortunately with unfavourable seasonal snow and some cloud cover over the area of interest. Imagery taken from the Space Shuttle such as the Metric Camera images of Soviet/Russian imagery such as KFA-1000 can provide additional information, if no other suitable imagery is available. The availability of Landsat data for free from the USGS archive and the ongoing acquisitions are of great value for glacier monitoring. Glacier changes exceeding 30 m can be detected using Landsat TM/ETM+, level 1T corrected from the USGS archive due to high precision of the orthorectification.

The automated generation of glacier drainage basins based on the SRTM3 data facilitated to split up contiguous ice masses into glaciers. However, we observed slight differences to some glaciers of the former Chinese Glacier Inventory. This led to different absolute areas for some glaciers, e.g. Zhadang Glacier (Chen et al., 2009). The area of the ice divide is almost flat in these cases. Further investigations, e.g. based on higher resolution DEMs, are required to identify the correct surface divide. This uncertainty does not affect the results of our study as we kept the ice divides constant for our analysis.

5.2 Glacier changes

The study reveals a long-term trend of glacier shrinkage and retreat in the western Nyainqentanglha Range since 1976. The slightly higher glacier shrinkage in Nam Co drainage basin compared to the whole study area is most likely due to the smaller average glacier size. Analysing the glacier hypsometry indicates that a rise of the ELA, which is currently estimated to be at ~5800 m, of more than 50 m will cause an increased area loss as the largest portion of glacier coverage is in the range of 5750–5850 m.

Our results are in line with previous studies. Field measurements and analysis of topographic maps carried out for Gurenhekou Glacier, located in southern part of the range, showed an increased termini retreat rate after 1970 (Pu et al., 2006). Similar analysis on five glaciers around Mt. Nyainqentanglha also suggests that glacier termini have been retreating around and above 10.0 m a-1 from 1970 to 2007, with a significant higher rate (~39 m/a) for debris-covered Xibu Glacier (Kang et al., 2007). Glacier mass balance measurements on Zhadang glacier show that negative balance values occur since 2005 except for a slight positive balance in 2008 (Zhou et al., 2007, Kang et al., 2009). Previous glacier-change studies for the Nam Co basin showed a glacier area decrease by 15.4% from 1970 to 2000 (Yao et al., 2007; Wu and Zhu, 2008) while Frauenfelder and Kääb (2009) found an area decrease of ~20% in the same period. This study, however, results in lower values for glacier area changes for a similar time period. Our results for length changes reveal similar values except for debris-covered Xibu Glacier. One reason for the differences could be that Yao et al., (2007) and Wu and Zhu (2008) used the data from the CGI (Li, 2003). This inventory used Chinese topographic maps (scale 1:100 000), which are based on aerial images acquired in the early 1970s, and were published in the 1970s and 1980s. The difference in retreat rates of debris-covered Xibu Glacier between this study and Kang et al. (2007) as well as the different delineation of the glaciers investigated in detail could also be caused by uncertain glacier outlines and ice divides obtained based on the 1970s maps. Frauenfelder and Kääb (2009) used Corona imagery to validate the data from the CGI and found errors in georeferencing which can be confirmed by this study. The authors omitted glaciers with obvious errors from the CGI for their change analysis but did not correct the remaining glaciers. Hence, the reason of the deviation to our data is likely due to the inaccurate 1970s data. Our results on area changes seem to be reliable as the area retreat is consistent with all utilized imagery. The quality of the CGI and Chinese topographic maps can hardly be evaluated if the original imagery is not available. Declassified imagery from the 1970s provides therefore a good opportunity for validation and to further improve the data from the CGI. Hexagon KH-9 data is superior to Corona due to less image distortion. However, topographic maps remain an important source for an estimate, if no other suitable data are available. This is especially true for the time prior the advent of satellite imagery.

Our results indicate that glacier changes in the western Nyainqentanglha Range are similar to the average changes for whole China (−5.5% since the 1960s, Li et al., 2008), and might be slightly higher than obtained values in other areas of central and western Tibet, e.g., the Geladanong Mountains ~500 km to the north of the study area (Ye et al., 2006, −4.8% between 1969 and 2002). Glacier shrinkage in Tibet south of the study area seems to be higher: Zhou et al., 2009 found a ~5% decrease between 1990 and 2005 in Nianchu River basin. However, these data can only show tendencies as different time periods and size classes are compared. Although glacier investigations and the availability of studies on glacier changes on the Tibetan Plateau increased in the recent years, a comprehensive overview taking different size classes, time periods, response times and climatic influences into account is still to be awaited.

None of the five glaciers that have been studied in detail deviates from the general trend of receding glaciers. Considering the strong small-scale climate variability of high-mountain regions it is remarkable that all the mean annual rates show comparable values, which indicates the dominant influence of long-term regional climate variability on glacier changes in the study area. The reported temperature increase since the 1950s varies between 0.3 K per decade for the station Lhasa, which was shown to be representative for a larger region (Liu and Chen, 2000). Frauenfeld et al. (2005) computed a trend of 0.14 K per decade in the Lhasa surroundings cells including Nam Co (period: 1958–2000) based on a comparison of gridded ERA-40 and station data. A recent study using similar data reveals also a general warming trend, especially in winter months (You et al., 2010). Whereas Liu and Chen (2000) assumed a higher increase in higher elevations, Qin et al. (2009) showed, by using remote sensing data, that this altitude trend may not be as strong as expected, and stagnates at elevations higher than 5000 m. These changes in air temperature are accompanied by an increase of precipitation due to variations in monsoonal activity. Zhao et al. (2004) noted an increase of annual precipitation of about 30 mm from 1967 to 1997 in south-eastern TiP, about 5.3% of the 31-year mean. Liu et al. (2009) analysed data of the station Amdo (~220 km in the NE), and recorded stable fluctuations in precipitation from 1965 to the mid-1990s, followed by an increasing trend since 1995. Annual precipitation in the last decade was 50.6 mm (about 12%) above the annual average during the period 1965–1994. The same tendency was observed by Shi et al. (2006) and Kang et al. (2007). Although a warming trend would cause continuous deficit glacier mass balance on the western Nyainqentanglha Range, precipitation seasonality also affects mass balance. For example, the early onset of rainy season may suppress glacier melt during the summer (Kang et al., 2009). So far, we are not able to attribute observed glacier changes to specific climate elements since availability of climatological data in the study area is insufficient, and present knowledge on the response of polythermal, summer-accumulation type glaciers to climate variability at different time scales is still limited. Ongoing investigations (e.g. mass balance measurements, meteorological measurements on Zhadang Glacier and Nam Co station, acquisition of gridded climate data) will continuously improve the data base in the near future.

One major impact of glacier recession in the study area is the increase of glacier meltwater runoff, which led into an increasing level of Nam Co (Wu and Zhu, 2008). This again led, and ongoing lake level rise will be leading to the loss of pasture land for the local population. The majority of the glaciers are part of the Brahmaputra River basin and hence, the knowledge on the glacier changes and its contribution to the river runoff is essential for many people not only in Tibet but also in India.

6 Conclusions

This study demonstrates the scientific value of detailed multi-temporal remote sensing analyses of glacier changes for regions that do not have sufficient observational data records. Our approach and the availability of precise orthorectified Landsat scenes allow repeated monitoring in the study area without costs for data every three to five years, if retreat rates remain unchanged. Human effort will be minor as glacier basins are already generated. The correction of the outlines derived in an automated manner would mainly concentrate on debris-cover correction. The availability of different optical satellite imageries from earlier years, especially the low cost Hexagon KH-9 from the 1970s and Landsat TM scenes from the 1980s and 1990s is of high value for glacier investigations. This allows evaluating existing data or glacier outlines from older topographic maps and deriving multi-temporal glacier inventories dating back several decades. In addition, this enables to show the consistency of the data. The main drawback for some regions might be the unavailability of suitable scenes. In our study area of continental climate, however, little snow cover and clouds throughout the year facilitated the generation of multi-temporal glacier inventories. The Chinese Glacier Inventory from the 1970 is a valuable source of information but the data has inaccuracies and geolocation errors. The use of different satellite data revealed a continuously glacier shrinkage of about 7.7% from 1976 until 2009. These values are lower than previously published results which can be mainly attributed to the uncertainties of glacier delineations based on the Chinese topographic maps. The five glaciers investigated in detail showed an average retreat of ~10 m/a from 1976 until 2009. No glaciers advanced in the investigated periods. The main cause of glacier wastage is likely the temperature increase but the complex glacier-climate interactions needs to be further investigated. In this respect the advent of gridded meteorological data sets derived from mesoscale reanalyses by numerical weather prediction models offers new possibilities, since data resulting from respective studies can be combined with the results achieved by this study. This kind of investigations is currently followed by the authors but will be subject of separate papers in the future.

Acknowledgements. The work is supported by the German Research Foundation (Deutsche Forschungsgemeinschaft, DFG) within the Tibetan Plateau (TiP) Priority Programme under the codes BU 949/20-1, SCHE 750/4-1, and SCHN 680/3-1. The authors are grateful to the German Aero Space Center (Deutsches Zentrum für Luft- und Raumfahrt, DLR) for providing the Metric Camera data at no cost. We thank Volker Hochschild, Jan Kropacek (both Universität Tübingen, Germany), Wolfgang Flügel, and Peter Krause (both Universität Jena, Germany) for the cooperation.

References

Ageta, Y. and Fujita, K.: Characteristics of mass balance of summer-accumulation type glaciers in the Himalayas and Tibetan Plateau, Zeitschrift für Gletscherkunde und Glazialgeologie 32, 61–65, 1996.

Ageta, Y. and Higuchi, K.: Estimation of mass balance components of a summer-accumulation type glacier in Nepal, Himalaya. Geogr. Ann. A, 66(3), 249–255, 1984.

Bajracharya, S. R. and Mool, P. K.: Glaciers, glacial lakes and glacial lake outburst floods in the Mount Everest region, Nepal., Ann. Glaciol. 50(53), 81–86, 2009.

Beniston, M.: Climatic Change in Mountain Regions: A Review of Possible Impacts. Clim. Change, 59, 5–31, 2003.

Bhambri, R. and Bolch, T.: Glacier Mapping: A Review with special reference to the Indian Himalayas, Prog. Phys. Geog., 33(5), 672–704, 2009.

Bolch, T., Buchroithner, M. F., Peters, J., Baessler, M., and Bajracharya, S.: Identification of glacier motion and potentially dangerous glacial lakes in the Mt. Everest region/Nepal using spaceborne imagery, Nat. Hazards Earth Syst. Sci., 8, 1329–1340, 2008, http://www.nat-hazards-earth-syst-sci.net/8/1329/2008/.

Bolch, T., Buchroithner, M. F., Pieczonka, T., and Kunert, A.: Planimetric and volumetric Glacier changes in Khumbu Himalaya since 1962 using Corona, Landsat TM and ASTER data, J. Glaciol. 54(187), 592–600, 2008b.

Bolch, T. and Kamp, U.: Glacier Mapping in High Mountains using DEMs, Landsat and ASTER Data. Grazer Schriften der Geographie und Raumforschung 41(=Proceedings of the 8th Int. Symp. on High Mountain Remote Sensing Cartography, 20–27 March 2005, La Paz, Bolivia), 13–24, 2006.

TCD

4, 429–467, 2010

Bolch, T., Menounos, B., and Wheate, R. D.: Landsat-based inventory of glaciers in western Canada, 1985–2005, Rem. Sens. Environ., 114(1), 127–137, 2010.
Braun, L., Weber, W., and M. Schulz, M.: Consequences of climate change for runoff from Alpine regions, Ann. Glaciol., 31, 19–25, 2000.
Chen, F., Kang, S., Zhang, J., You, Q.: Glaciers and lake change in response to climate change in the Nam Co Basin, Tibet (in Chinese with English abstract), Journal of Mountain Sciences, 27(6), 641–647, 2009.
Ding, Y., Liu, S., Li, J., and Shangguan, D.: The retreat of glaciers in response to recent climate warming in western China, Ann. Glaciol., 43, 97–105, 2006.
Falorni, G., Teles, V., Vivoni, E. R., Bras, R. L., and Amartunga, K. S. Analysis and characterization of the vertical accuracy of digital elevation models from the Shuttle Radar Topography Mission, J. Geophys. Res., 110, F02005, doi:10.1029/2003JF000113, 2005.
Frauenfeld, O. W., Zhang, T., and Serreze, M. C.: Climate change and variability using European Centre for Medium-Range Weather Forecasts reanalysis (ERA-40) temperatures on the Tibetian Plateau, J. Geophys. Res., 110(D02101), doi:10.1029/2004JD005230, 2005.
Frauenfelder, R. and Kääb, A.: Glacier mapping from multi-temporal optical remote sensing data within the Brahmaputra river basin. Proc. 33rd int. Symposium on Remote Sensing of Environment, 4–8 May 2009, Stresa, Italy. Tucson, Arizona: International Center of Remote Sensing of Environment, Paper 299, pp. 4, 2009.
Fujita, K. and Ageta, Y.: Effect of summer accumulation on glacier mass balance on the Tibetan Plateau revealed by mass-balance model, J. Glaciol., 46(153), 244–252, 2000.
Fujita, K., Ohta, T., and Ageta, Y.: Characteristics and climatic sensitivities of runoff from a cold-type glacier on the Tibetan Plateau, Hydrol. Proc., 21, 282–2891, 2007.
Fujita, K., Seko, K., Ageta, Y., Pu, J., and Yao, T.: Superimposed ice in glacier mass balance on the Tibetan Plateau, J. Glaciol., 42(142), 454–460, 1996.
Granshaw, F. D. and Fountain, A. G.: Glacier change (1958–1998) in the North Cascades National Park Complex, Washington, USA, J. Glaciol., 52(177), 251–256, 2006.
Haeberli, W. and Beniston, M.: Climate Change and its impacts an glaciers and permafrost in the Alps. Ambio, 27(4), 258–265, 1998.
Hagg, W., Braun, L., Weber, M., and Becht, M.: Runoff modelling in glacierized Central Asian catchments for present-day and future climate, Nordic Hydol., 332(1–2), 40–53, 2007.
Huang, M.: On the temperature distribution of glaciers in China, J. Glaciol., 36(123), 210–216, 1990.

Kamp, U., Bolch, T., and Olsenholler, J.: Geomorphometry of Cerro Sillajhuay, Chile/Bolivia: comparison of DEMs derived from ASTER remote sensing data and contour maps. Geocarto International, 20(1), 23-34, 2005.

Kang S., Wei, X., You, Q., Flügel, W., Pepin, N., and Yao, T.: Review of climate and cryospheric change in the Tibetan Plateau, Environ. Res. Lett., 5, 015101, 8 pp., doi:10.1088/1748-9326/5/1/015101, 2010.

Kang, S., Chen, F., Gao, T., Zhang, Y., Yang, W., Yu, W., and Yao, T.: Early onset of rainy season suppresses glacier melt: a case study on Zhadang glacier, Tibetan Plateau, J. Glaciol., 55(192), 755–758, 2009.

Kang, S., Chen, F., Ye, Q., Jing, Z., Qin, D., and Ren, J.: Glacier retreating dramatically on Mt. Nyainqêntanglha during the last 40 years. (in Chinese with English summary), J. Glaciol. Geocryol., 29(6), 869–873, 2007.

Kang, S., Qin, D., Ren, J., Zhang, Y., Kaspari, S., Mayewski, P. A., and Hou, S.: Annual accumulation in the Mt. Nyainqentanglha ice core, southern Tibetan plateau, China: Relationships to atmospheric circulation over Asia, Arct. Antarct. Alp. Res., 39, 663–670, 2007.

Konecny, G., Reynolds, M., and Schroeder, M.: Mapping from Space: The Metric Camera experiment, Science, 225(4658), 167–169, 1984.

Li, X.: GLIMS Glacier Database. Boulder, CO, National Snow and Ice Data Center/World Data Center for Glaciology, Digital Media, 2003.

Li, X., Cheng, G., Jin, H., Kang, E., Che, T., Jin, R., Wu, L., Nan, Z., Wang, J., and Shen, Y.: Cryospheric change in China, Global Planet. Change, 62(3–4), 210–218, 2008.

Liu, J., Wang, S. Yu, S., Yang, D., and Zhang, L.: Climate warming and growth of high-elevation inland lakes on the Tibetan Plateau, Global Planet. Change, 67, 209–217, 2009.

Liu, X. and Chen, B.: Climatic warming in the Tibetan Plateau during recent decades, Int. J. Climate, 20(14), 1729–1742, 2000.

Ma, D., Tu, J., Cui, P., and Lu, R.: Approach to Mountain Hazards in Tibet, China, J. MT. Sci., 1(2), 143–154, 2004.

Narama, C., Shimaura, Y., Nakayama, D., and Abdrakhmatov, K. E.: Recent Changes of Glacier Coverage in the Western Terskey-Alatoo Range, Kyrgyz Republic, using Corona and Landsat, Ann. Glaciol., 43, 223–229, 2006.

Paul, F. R., Barry, R. G., Cogley, J. G., Haeberli, W., Ohmura, A., Ommanney, C. S. L., Raup, B., Rivera, A., and Zemp, M.: Recommendations for the compilation of glacier inventory data from digital sources, Ann. Glaciol., 50(53), 119–126, 2009.

Paul, F., A. Kääb, A., Maisch, M., Kellenberger, T., and Haeberli, W.: The new remote sensing derived Swiss Glacier Inventory: I. Methods. Ann. Glaciol., 34, 355-361, 2002.
Pu, J., Yao, T., and Tian, L.: Change of the Gurenhekou Glacier in Yangbajain Area, Nyainqêntanglha Range, J. Glaciol. Geocryol., 28(6), 861–864, 2006.
Qin, J., Yang, K., Liang, S., and Guo, X.: The altitudinal dependence of recent rapid warming over the Tibetan Plateau, Climatic Change, 97(1–2), 321–327, 2009.
Ren, J., Jiang, C., Zhang, Z., Qin, D., and Huang, J.: Geotectonic evolution of China. Science Press Beijing. Berlin, Heidelberg, New York, London, Paris, Tokio, 203 p., 1987.
Richardson, S. D. and Reynolds, J. M.: An overview of glacial hazards in the Himalayas, Quatern. Int., 65/66(1), 31–47, 2000.
Sato, T.: Spatial and temporal variations of frozen ground and snow cover in the eastern part of the Tibetan Plateau, J. Meteorol. Soc. Jpn., 79(1B), 519–534, 2001.
Schiefer, E., Menounos, B., and Wheate, R. D.: An inventory and morphometric analysis of British Columbia glaciers, Canada, J. Glaciol., 54(186), 551–560, 2008.
Schütt, B., Berking, J., Frechen, M., and Yi, C.: Late Pleistocene Lake Level Fluctuations of the Nam Co, Tibetan Plateau, China, Zeitschrift für Geomorphologie, Supplementary Issues, 52(2), 57–75, 2008.
Shi, Y., Hsieh, T., Chen, P., and Li, C. Distribution, features and variation of glaciers in China, IAHS Publ., 126, 111–116, 1980.
Shi, Y. and Liu, S.: Estimation on the response of glaciers in China to the global warming in the 21st century, Chinese Sci. Bull., 45(7), 668–672, 2000.
Shi, Y., Liu, S., Shangguan, D., Li, D., and Ye, B.: Peculiar phenomena regarding climatic and glacial variations on the Tibetan Plateau, Ann. Glaciol., 43, 106–110, 2006.
Surazakov, A. B. and Aizen, V. B.. Positional accuracy evaluation of declassified Hexagon KH-9 mapping camera imagery. Photogrammetric Engineering and Remote Sensing, accepted, 2010.
Toutin, T.: ASTER DEMs for geomatic and geoscientific applications: a review, Int. J. Remote Sens., 29(7), 1855–1875, 2008.
Tucker, C., Grant, D., and Dykstra, J.: NASA's global orthorectified Landsat data set. Photogrammetric Engineering and Remote Sensing, 70(3), 313–322, 2004.
Wu, Y. and Zhu, L.: The response of lake-glacier variations to climate change in Nam Co Catchment, central Tibetan Plateau, during 1970-2000. J. Geogr. Sci., 18(2), 177–189, 2008.
Xiao, C., Liu, S., Zhao, L., Wu, Q., Li, P., Liu, C., Zhang, Q., Ding, Y., Yao, T., Li, Z., and Pu,

J.: Observed changes of cryosphere in China over the second half of the 20th century: an overview, Ann. Glaciol., 46, 382–390, 2007.
Yang, Z., Cheng, Y., and H. Wang, H.: The geology of China, Oxford Monographs on Geology and Geophysics, 3, Allen, P., Oxburgh, E. R., and Skinner, B. J., Clarendon Press, Oxford, 1986.
Yao, T.: Map of Glaciers and Lakes on the Tibetan Plateau and Adjoining Regions 1:2 000 000, Xian Cartographic Publishing House, 2008.
Yao, T., Pu, J., Lu, A., Wang, Y., and Yu, W.: Recent glacial retreat and its impact on hydrological processes on the Tibetan Plateau, China, and surrounding regions, Arct. Antarct. Alp. Res., 39(4), 642–650, 2007.
Ye, Q., Kang, S. Chen, F., and Wang, J.: Monitoring glacier variations on Geladandong Mountian, central Tibetan Plateau, from 1969 to 2002 using remote-sensing and GIS technologies, J. Glaciol., 52(179), 537–545, 2006.
You, Q., Kang, S., Tian, K., Liu, J., Li, C., and Zhang, Q.: Preliminary analysis on climatic features at Mt. Nyainqentanglha, Tibetan Plateau (in Chinese with English abstract), J. MT. Sci., 25(4), 497–504, 2007.
You Q., Kang, S., Aguilar, E., Flügel, W., and Yan, Y.: Relationship between temperature trend magnitude, elevation and mean temperature in the Tibetan Plateau from homogenized surface stations and reanalysis data, Global Planet. Change, 71(1-2), 124–133, doi:10.1016/j.gloplacha2010.01.20, 2010.
Zhang, Y., Kang, S., and Li, M.: Climatic features at Nam Co station, Tibetan Plateau (in Chinese with English abstract), Annual Report of Nam Co Station for Multisphere observation and Research, 3, 1–8, 2008.
Zhao, L., Ping, C., Yang, D., Cheng, G., Ding, Y., and Liu, S.: Changes of climate and seasonally frozen ground over the past 30 years in Qinghai-Xizang (Tibetan) Plateau, China, Global Planet. Change, 43, 19–31, 2004.
Zhou, C., Yang, W., Wu, L., and Liu, S.: Glacier changes from a new inventory, Nianchu river basin, Tibetan Plateau, Ann. Glaciol., 50(53), 87–92, 2009.

Table 1. Utilized space imagery.

Date	Satellite and Sensor	Path/Row	Resolution	Spectral Bands
21/11/70	Corona KH-4B		~4 m, stereo	1 PAN
07/01/76	Hexagon KH-9		~8 m, stereo	1 PAN
7/12/76	Landsat MSS		79 m	3 VIS, 1 NIR
23/11/84	Space Shuttle Metric Camera		~16 m, stereo	1 VIS
14/09/91	Landsat TM	138/039	30 m	3 VIS, 1 NIR, 2 SWIR, 1 TIR
17/11/00	Landsat ETM+	138/039	15/30 m	1 PAN, 3 VIS, 1 NIR, 2 SWIR, 1 TIR
02/05/01	Landsat ETM+	138/039	15/30 m	1 PAN, 3 VIS, 1 NIR, 2 SWIR, 1 TIR
06/12/01	Landsat ETM+	138/039	15/30 m	1 PAN, 3 VIS, 1 NIR, 2 SWIR, 1 TIR
20/01/01	Terra ASTER		15/30 m, stereo	2 VIS, NIR, TIR
07/10/05	Landsat ETM+, SLCoff	138/039	15/30 m	1 PAN, 3 VIS, 1 NIR, 2 SWIR, 1 TIR
18/01/06	Landsat ETM+, SLCoff	138/039	15/30 m	1 PAN, 3 VIS, 1 NIR, 2 SWIR, 1 TIR
23/01/06	SPOT2C		20 m	3 VIS
01/08/07	Landsat ETM+, SLCoff	138/038	15/30 m	1 PAN, 3 VIS, 1 NIR, 2 SWIR, 1 TIR
06/01/08	Landsat ETM+, SLCoff	138/039	15/30 m	1 PAN, 3 VIS, 1 NIR, 2 SWIR, 1 TIR
19/06/09	Landsat ETM+, SLCoff	138/039	15/30 m	1 PAN, 3 VIS, 1 NIR, 2 SWIR, 1 TIR
21/07/09	Landsat ETM+, SLCoff	138/039	15/30 m	1 PAN, 3 VIS, 1 NIR, 2 SWIR, 1 TIR
15/09/09	Landsat TM	138/039	30 m	3 VIS, 1 NIR, 2 SWIR, 1 TIR

Table 1. Continued.

Source	Suitability of scene	Utilisation
USGS		Additional information for glacier identification
USGS		Glacier inventory ∼1976 for whole study area
GLCF		Glacier inventory ∼1976 for whole study area
DLR	Seasonal snow on glaciers	Additional information for selected glaciers
GLCF	Seasonal snow on glaciers	Length changes
USGS		Glacier inventory ∼2001, for whole study area
USGS		Glacier inventory ∼2001, additional information
USGS		Glacier inventory ∼2001, additional information
USGS		Glacier inventory ∼2001 additional information
USGS		Additional information for selected glaciers
USGS		Additional information for selected glaciers
GAF		Additional information for selected glaciers
USGS		Glacier inventory north-eastern part
USGS		Glacier inventory ∼2009 for the detailed study area
USGS	Some clouds	Glacier inventory ∼2009 for the detailed study area
USGS		Glacier inventory ∼2009 for the detailed study area
USGS	Some clouds	Glacier inventory ∼2009 for the detailed study area

TCD
4, 429–467, 2010

Title Page
Abstract Introduction
Conclusions References
Tables Figures
◂ ▸
Back Close
Full Screen / Esc
Printer-friendly Version
Interactive Discussion

Table 2. Number and ice covered area of the study areas based on the glacier inventory.

	Number	Area (km^2)
Whole Mountain range	963	795.6 ± 22.3
North-eastern section	141	103.2 ± 2.9 (year 2009)
South-western section	822	692.3 ± 19.4 (2001)
Nam Co drainage basin	305	198.1 ± 5.6
Area around Mt. Nyainqentanghla	308	196.2 ± 5.5

Table 3. Characteristics of the glaciers investigated in detail based on the 2001 extends.

Glacier	GLIMS ID/WGI ID*	Area (km^2)	Length (km)	Aspect	H med[1] (m a.s.l.)	H min[2] (m a.s.l.)	H max[3] (m a.s.l.)	Debris-covered tongue
Zhadang	G090633E30476N/ 5Z225D0003	2.48	2.7	NE	5710	5500	6095	No
Tangse No. 2	G090647E30462N/ 5O270C0086	2.96	2.1	SW	5785	5600	6080	No
Lalong	G090540E30424N/ 5Z225D0022	10.29	3.6	NW	5890	5340	6650	Few medial moraines
Xibu	G090601E30395N/ 5O270C0065	23.35	9.3	E	5815	5160	7090	Yes
Panu	G090521E30384N/ 5O270C0044	12.88	5.3	SE	5850	5335	6365	Few medial moraines

* ID number of the GLIMS data base (Li, 2003, www.glims.org) and the World Glacier Inventory (www.wgms.ch),
[1] median elevation,
[2] minimum elevation,
[3] maximum elevation

TCD
4, 429–467, 2010

Table 4. Change in glacier area 1976–2001–2009.

	Area [km^2]			1976–2001		
	1976	2001	2009	Δa [km^2]	Δa [%]	Δa/yr. [%]
South-western Area	734.1 ± 25.7	692.4 ± 19.4	n.a.	−41.7 ± 22.4	−5.7 ± 3.1	−0.23 ± 0.12
Nam Co Basin	212.5 ± 7.4	198.1 ± 5.5	n.a.	−14.4 ± 6.5	−6.8 ± 3.1	−0.27 ± 0.12
Area around Mt. Nyainqen-tanghla	207.1 ± 7.2	196.2 ± 5.5	191.1 ± 5.4	−10.9 ± 6.4	−5.3 ± 3.1	−0.21 ± 0.12

Table 4. Continued.

	2001–2009			1976–2009		
	Δa [km^2]	Δa [%]	Δa/yr. [%]	Δa [km^2]	Δa [%]	Δa/yr. [%]
South-western Area	n.a.	n.a.	n.a.	n.a.	n.a.	n.a.
Nam Co Basin	n.a.	n.a.	n.a.	n.a.	n.a.	n.a.
Area around Mt. Nyainqen-tanghla	-5.1 ± 5.4	-2.6 ± 2.8	-0.33 ± 0.34	-16.0 ± 6.4	-7.7 ± 3.1	-0.23 ± 0.10

Table 5. Length and area changes for five selected glaciers.

Zhadang Glacier	Area (km^2)	Δa abs. (km^2)	Δa rel. (km^2)	Rate (%/a)	Retreat (m)	Rate (m/a)
1976	2.75					
1991	2.56	−0.19	−6.9%	−0.46%	140	9.3
2001	2.48	−0.08	−3.1%	−0.31%	70	7.0
2005	2.41	−0.07	−2.8%	−0.71%	40	10.0
2009	2.36	−0.05	−2.1%	−0.52%	45	11.3
1976–2001		−0.27	−9.8%	−0.39%	210	8.4
2001–2009		−0.12	−4.8%	−0.60%	85	10.6
1976–2009		−0.39	−14.2%	−0.43%	295	8.9
Tangse Glacier No. 2	Area (km^2)	Δa abs. (km^2)	Δa rel. (km^2)	Rate (%/a)	Retreat (m)	Rate (m/a)
1976	3.13					
1991	3.02	−0.11	−3.5%	−0.23%	70	4.7
2001	2.96	−0.06	−2.0%	−0.20%	65	6.5
2005	2.95	−0.01	−0.3%	−0.08%	30	7.5
2009	2.89	−0.06	−2.0%	−0.51%	35	8.8
1976–2001		−0.17	−5.4%	−0.22%	135	5.4
2001–2009		−0.07	−2.4%	−0.30%	65	8.1
1976–2009		−0.24	−7.7%	−0.23%	200	6.1
Lalong Glacier	Area (km^2)	Δa abs. (km^2)	Δa rel. (km^2)	Rate (%/a)	Retreat (m)	Rate (m/a)
1976	10.5					
1984	10.43	−0.07	−0.7%	−0.08%	170	21.3
2001	10.29	−0.14	−1.3%	−0.08%	190	11.9
2005	10.25	−0.04	−0.4%	−0.10%	60	15.0
2009	10.24	−0.01	−0.1%	−0.02%	15	3.8
1976–2001		−0.21	−2.0%	−0.08%	360	14.4
2001–2009		−0.05	−0.5%	−0.06%	75	9.4
1976–2009		−0.26	−2.5%	−0.08%	435	13.2
Xibu Glacier	Area (km^2)	Δa abs. (km^2)	Δa rel. (km^2)	Rate (%/a)	Retreat (m)	Rate (m/a)
1976	23.55					
1984	23.43	−0.12	−0.5%	−0.06%	120	15.0
1991	23.39	−0.04	−0.2%	−0.02%	50	7.1
2001	23.35	−0.04	−0.2%	−0.02%	60	6.0
2005	23.04	−0.5	−2.1%	−0.33%	50	12.5
2009	22.90	−0.14	−0.6%	−0.15%	50	12.5
1976–2001		−0.2	−0.9%	−0.03%	230	9.2
2001–2009		−0.36	−1.5%	−0.24%	100	12.5
1976–2009		−0.44	−1.9%	−0.07%	330	10.0
Panu Glacier	Area (km^2)	Δa abs. (km^2)	Δa rel. (km^2)	Rate (%/a)	Retreat (m)	Rate (m/a)
1976	13.18					
1984	13.16	−0.02	−0.2%	−0.02%	100	12.5
1991	13.01	−0.15	−1.1%	−0.16%	80	11.4
2001	12.88	−0.13	−1.0%	−0.06%	190	19.0
2005	12.86	−0.02	−0.2%	−0.04%	70	17.5
2009	12.78	−0.08	−0.6%	−0.16%	30	7.5
1976–2001		−0.3	−2.3%	−0.09%	370	14.8
2001–2009		−0.1	−0.8%	−0.10%	100	12.5
1976–2009		−0.38	−2.9%	−0.09%	470	14.2

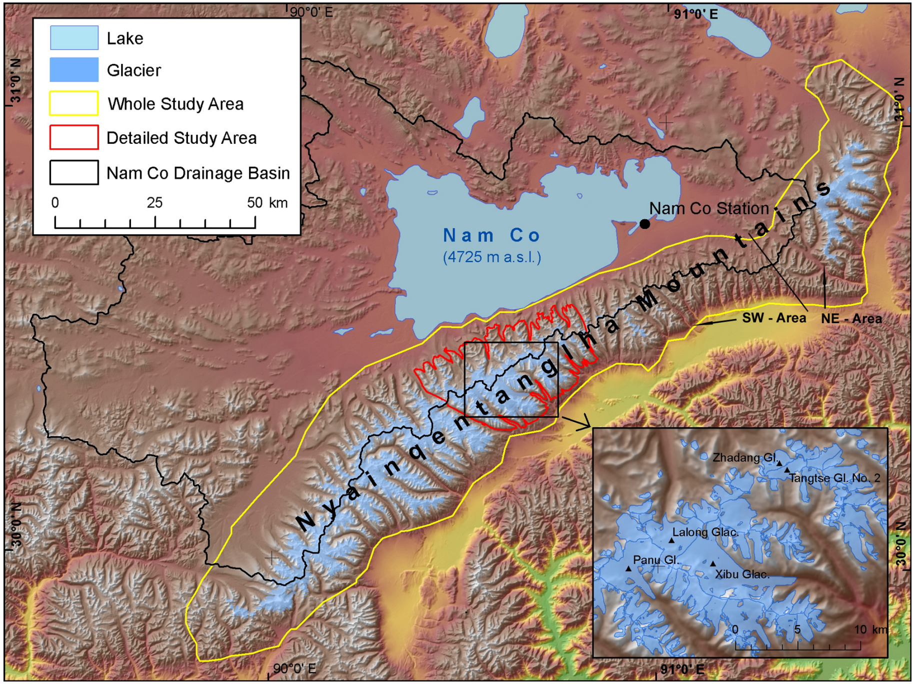

Fig. 1. Overview of the study area.

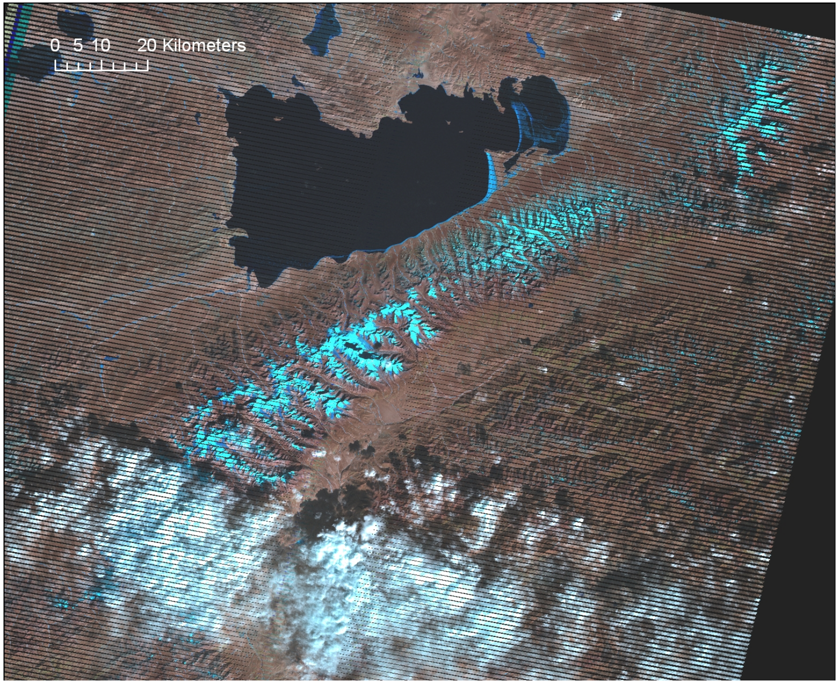

Fig. 2. Typical situation of a Landsat scene (ETM+ SLC-off from 18/01/2006): Part of the study area is suitable for glacier mapping, while seasonal snow hampers correct mapping in the NE region, and clouds covers the SW region. The region of highest interest in the center is not affected by scanline errors of the SLC scene.

TCD

4, 429–467, 2010

A glacier inventory for the western Nyainqentanglha Range

T. Bolch et al.

Fig. 3. Terminus of debris-covered Xibu Glacier; Corona (year 1970, **A**), Hexagon (1976, **B**), Landsat ETM+, 5-4-3-pan (2009, **C**).

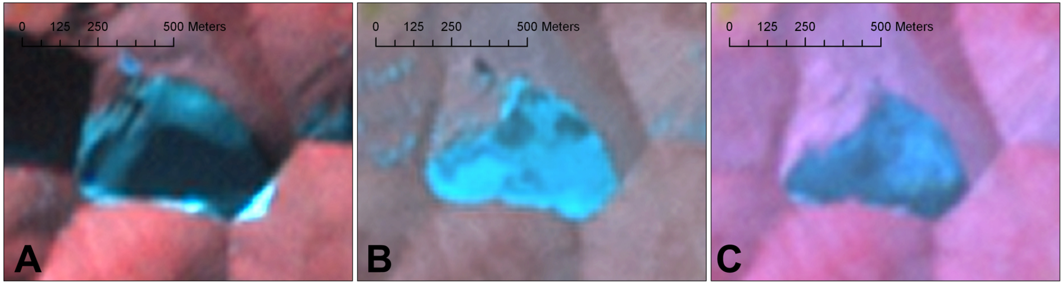

Fig. 4. Small glacier on three different images: 06/12/2001 **(A)**, 19/06/2009 **(B)**, and 21/07/2009 **(C)**; B and C illustrate the influence of different snow conditions on delineated glacier outlines.

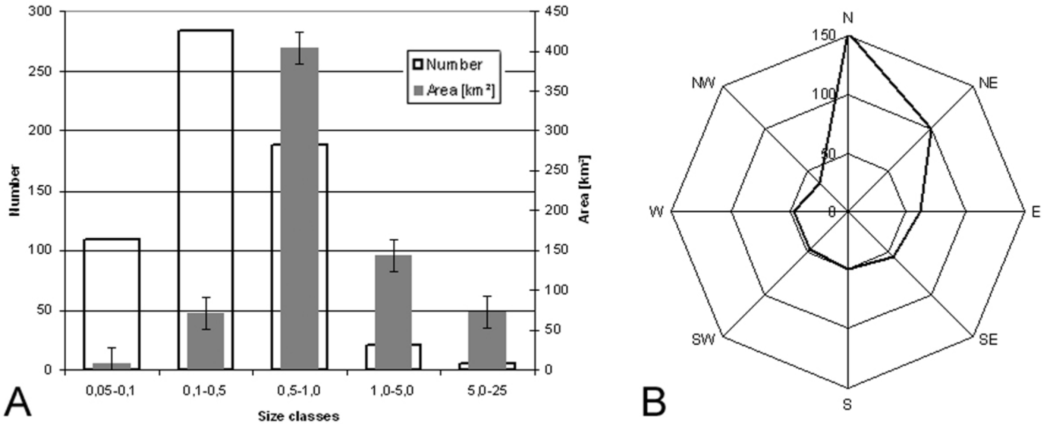

Fig. 5. (A): Diagram showing the number and covered area for different size classes, **(B):** aspect of the glaciers in the study area.

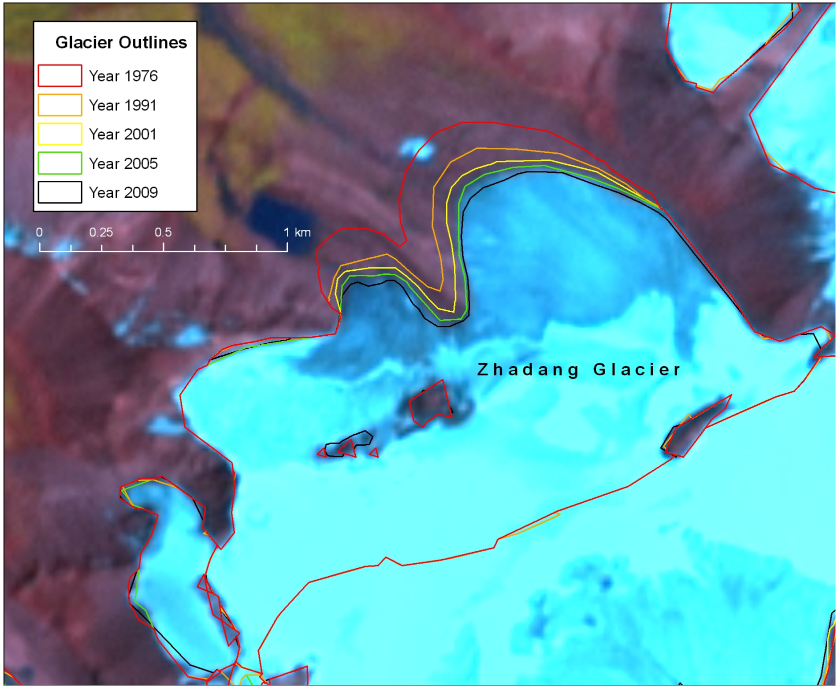

Fig. 6. Area changes of Zhadang Glacier (1976–2009).

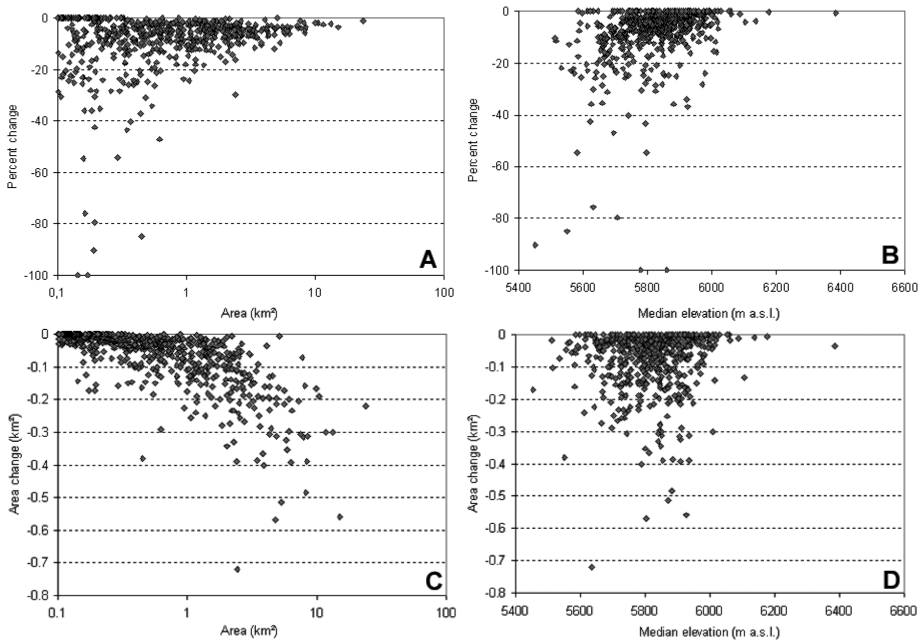

Fig. 7. Relative change in glacier area 1976–2001 versus initial glacier area **(A)** and median elevation **(B)**, absolute change in glacier area 1976–2001 versus initial glacier area **(C)** and median elevation **(D)**.

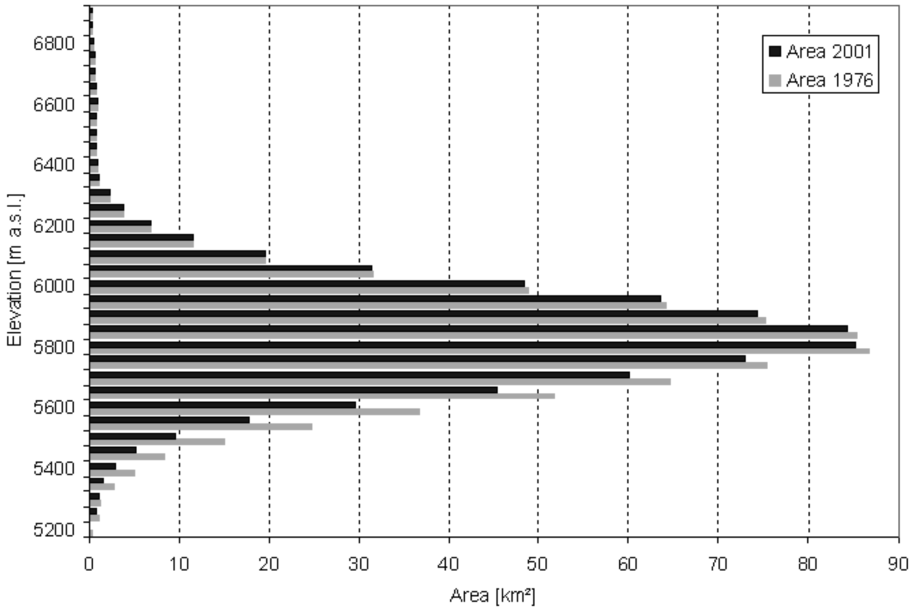

Fig. 8. Changes in glacier hypsometry 1976–2001; each bar represents an elevation interval of 50 m.

TCD

4, 429–467, 2010

A glacier inventory for the western Nyainqentanglha Range

T. Bolch et al.

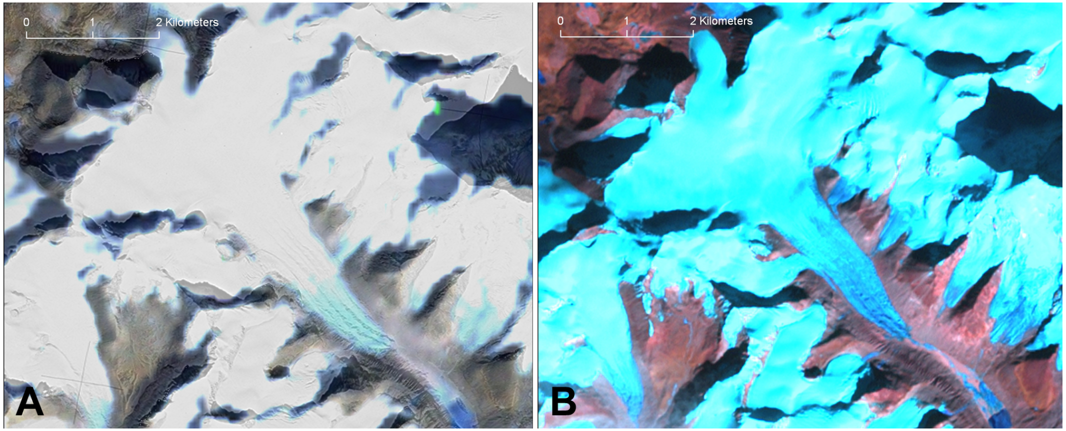

Fig. 9. Panu Glacier 1976 (merge of Landsat MSS and Hexagon), **(A)**, and 2001 (Landsat ETM+, 5-4-3-PAN), **(B)**.